Available online at www.sciencedirect.com

ScienceDirect

Mendeleev Commun., 2020, **30**, 580–582

Mendeleev Communications

Structure-defining interactions in the salt cocrystals of $[(Me_5C_5)_2Fe]^+I_3^-$–XC_6H_4OH (X = Cl, I): weak noncovalent *vs.* strong ionic bonding

Yury V. Torubaev,*[a] Ivan V. Skabitsky[a] and Konstantin A. Lyssenko[b,c]

[a] *N. S. Kurnakov Institute of General and Inorganic Chemistry, Russian Academy of Sciences, 119991 Moscow, Russian Federation. E-mail: torubaev@igic.ras.ru*
[b] *G. V. Plekhanov Russian University of Economics, 117997 Moscow, Russian Federation*
[c] *Department of Chemistry, M. V. Lomonosov Moscow State University, 119991 Moscow, Russian Federation*

DOI: 10.1016/j.mencom.2020.09.009

In the cocrystalline salts $[(Me_5C_5)_2Fe^+]I_3^-/(4\text{-}XC_6H_4OH)$ (X = = Cl, I), the directionality of X···I–I_2 halogen bonds is a significant packing factor notwithstanding their relatively low energies (~10 kcal mol^{-1}), as compared to the fivefold stronger ionic bonding between $[(Me_5C_5)_2Fe^+]$ and $[I_3]^-$ (~50 kcal mol^{-1}). This adds significant details to the structural landscape of $[(Me_5C_5)_2Fe^+]I_3$ and offers an illustrative example of the stronger structure-defining effect of halogen bonding over the hydrogen one.

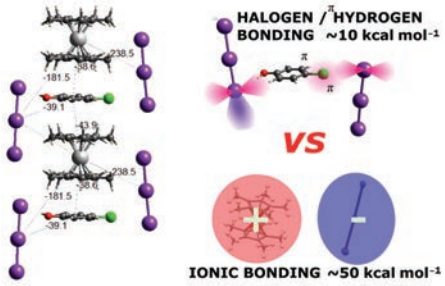

Keywords: halogen bonding, hydrogen bonding, ternary crystals, cocrystals, ferrocene, ferrocenyl, polyiodide, intermolecular interactions, supramolecular.

The classification of ionic cocrystals was a subject for some controversy[1] and a transition from cocrystals to salts in certain ternary systems was shown to be continuous.[2] Currently, the formal ternary system [A$^-$]–B–[C$^+$] (A is an anion, C is a cation, and B is a neutral molecule) can be clearly defined as salt cocrystals.[3] In the same way as binary molecular cocrystals expand the structural landscapes of their parent co-formers,[4] the binary cocrystalline salts [A$^-$]–B–[C$^+$] may shed light on the structural landscapes of the ionic pairs [A]$^-$[C$^+$]. With this in mind, we studied the supramolecular reactions of organometallic salts with neutral organic co-formers capable of forming or stabilizing layered, porous, cage and other stable supramolecular architectures, *i.e.* long range aufbau supramolecular synthon modules (LSAMs),[4,5] which are the stable assemblies of supramolecular synthons.[6] Particularly, polyiodide anions were successfully used in the design of 3D molecular architectures assisted by specific and directional CH---I and I---N noncovalent interactions.[7,8]

We studied the interaction of decamethylferrocenium (DMFc) salts with organic porous compounds. In case of $[DMFc]^+I_3^-$ (refs. 9,10) and 1,3,5-$C_3N_3(OC_6H_4X)_3$ (X = Cl, I) (ref. 11), we did not obtain expected host–guest cocrystals, but we isolated the cocrystal of $[DMFc]^+I_3$ and 1,4-ClC_6H_4OH as a new solid-state product (**1**) [Figure 1(*a*)]. The appearance of 4-ClC_6H_4OH can be easily traced as it was the starting material for 1,3,5-$C_3N_3(OC_6H_4Cl)_3$, and the samples of $C_3N_3(OC_6H_4Cl)_3$ may have a characteristic phenolic odor of 4-ClC_6H_4OH even after thorough washing.

As expected, **1** was formed almost quantitatively upon the cocrystallization of corresponding amounts of DMFc, I_2 and

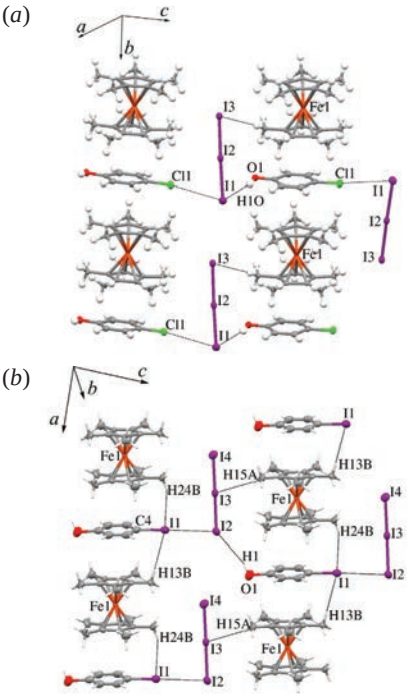

Figure 1 Fragments of (*a*) **1** and (*b*) **2** crystal packing showing the OH···I_3 HB, Cl···I_3 and I···I_3 XB interactions (thermal ellipsoids at a 50% probability level). Selected distances (Å) in **1**: I1–I2, 2.9411(7); I2–I3, 2.9307(6); H1O–I1, 2.6608; and I1–Cl1, 3.772(3). Angles (°): C21–Cl1–I1, 171.8(3); I2–I1–Cl1, 73.39(4); and I2–I1–H1O, 75.61. Selected distances (Å) in **2**: I4–I3, 2.9073(5); I3–I2, 2.9131(5); I1–I2, 3.7693(5); and H1–I2, 3.2987. Angles (°): C4–I1–I2, 175.9(1); I3–I2–I1, 86.94(1); and I3–I2–H1, 133.44.

4-ClC_6H_4OH.† Its solid-state structure‡ can be described as parallel chains of discrete I_3 anions and the stacks of alternating 4-ClC_6H_4OH and DMFc, which are interconnected by CH···I and OH···I hydrogen bonds (HBs) (Figures 1 and 2). Under the same conditions, *p*-iodophenol (4-IC_6H_4OH) afforded similar (but not isomorphic) cocrystals of [DMFc]I_3(4-IC_6H_4OH) (**2**) [Figure 1(*b*)]. Computational analysis of intermolecular interactions in **1**, **2** (TONTO/CE-B3LYP-DGDZP)[8] showed that dispersion forces contribute significantly to the Cp*···4-XPhOH [X = Cl (**1**), I (**2**)] π–π stacking only, while OH···I HBs in **1**, **2** are mostly electrostatically driven.§

Competition and complex interplay of XB *vs*. HB has been of particular interest in the past decade.[12,13] The Cl function in 4-ClC_6H_4OH is very poor XB donor, so the Cl···I XB is absent from **1** and I_3···ClC_6H_4OH interaction appears repulsive (+4.3 kJ mol^{-1}).¶ Consequently, the mutual arrangement of I_3 and 4-ClC_6H_4OH favors not the I···Cl XB but rather effective O–H···I–I_2 HB (Figure 3). This HB also appears stronger (–39 kJ mol^{-1}) than O–H···I–I_2 HB in **2** (–25.8 kJ mol^{-1}). In the latter, the direction of σ-hole on the iodine in 4-IC_6H_4OH and the nucleophilic area of the terminal iodine in I_3^- favor the type-II (genuine) XB[14] I···I (–11 kJ mol^{-1}). This occurs at the expense of weakening of O–H···I–I_2 HB, where the OH hydrogen atom is directed towards the electrophilic area of terminal iodine in I_3^- (see Figures 1 and 3). Additionally, the absence of strong H-bonds from **2** is probably a reason for the slight (~3.5%) X/OH (X = I) disorder, which was observed in **2**§ but was not noticed in **1**.

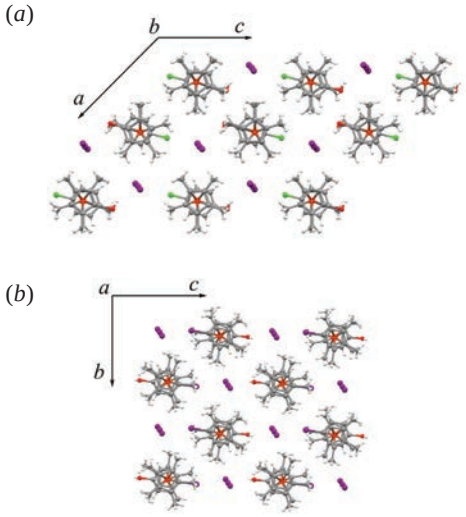

Figure 2 Fragments of crystal packing of (*a*) **1** (*C*2/*c*, view along the *b* axis) and (*b*) **2** ($P\bar{1}$, view along the *a* axis).

Although both **1** and **2** demonstrate general similarity of packing patterns, their crystals are not isostructural, and the geometry of these I···I, Cl···I XBs and OH···I HBs makes a difference between them. We have already described and analyzed in detail the difference in the geometry of XBs between metal halide XB acceptors with iodoorganic XB donors.[15,16] In case of **1** and **2**, the same scenario repeats, so that iodine XB acceptor dictate the 90° angle for XB, while chlorine, being a negative sphere without pronounced directionality, results in repulsive interaction with the I_3 anion (+4 kJ mol^{-1}) (see Figure 3).§

The geometry of structures **1** and **2** is in good agreement with the conditions of the formation of ternary crystals:[17] indeed, the introduction of a third component (4-XC_6H_4OH, X = Cl, I) adds

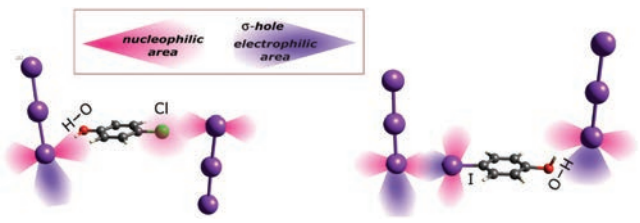

Figure 3 Fragments of the solid state structures of **1** and **2** showing electrophilic (σ-hole) and nucleophilic areas associated with halogen atoms and the directionality of I···I XBs and OH···I HBs. Note that the hydroxyl hydrogen in **1** is directed towards the nucleophilic area of terminal iodine of the I_3 anion, while the hydroxyl hydrogen in **2** is missing the nucleophilic area of terminal iodine of the I_3 anion.

† Solvents were purified, dried, and distilled under an argon atmosphere before use. Commercial iodine, $(Me_5C_5)_2Fe$, 4-ClC_6H_4OH, and 4-IC_6H_4OH were used without additional purification.

Preparation of [$(Me_5C_5)_2Fe$]-I_3-(4-ClC_6H_4OH) **1**. ($Me_5C_5)_2Fe$ (8 mg, 0.025 mmol) and I_2 (10 mg, 0.04 mmol) were dissolved in CH_2Cl_2 (0.1 ml) in a 5 mm glass tube, and 4-ClC_6H_4OH (4 mg, 0.03 mmol) was added to the green solution. The color of the reaction mixture turned brown, and the tube was sealed with two layers of parafilm and left at room temperature in the dark. Slow diffusion of the solvent through the parafilm for five days afforded well-formed uniform dichroic brownish green plates, which were washed with hexane, dried, and used for single crystal XRD analysis. Yield, 20 mg (96%).

Preparation of [$(Me_5C_5)_2Fe$]-I_3-(4-IC_6H_4OH) **2**. ($Me_5C_5)_2Fe$ (8 mg, 0.025 mmol) and I_2 (10 mg, 0.04 mmol) were dissolved in CH_2Cl_2 (0.1 ml) in a 5 mm glass tube and 4-IC_6H_4OH (6 mg, 0.027 mmol) was added to the green solution. The color of the reaction mixture turned brown. Treatment similar to the above one afforded well-formed uniform dichroic brownish green plates, which were washed with hexane, dried, and used for single crystal XRD analysis**.** Yield, 21 mg (91%).

Preparation of [$(Me_5C_5)_2Fe$]-I_3 **3**. ($Me_5C_5)_2Fe$ (8 mg, 0.025 mmol) and I_2 (10 mg, 0.04 mmol) were dissolved in 0.2 ml of CH_2Cl_2 in a 5 mm glass tube. Analogous treatment afforded well-formed uniform dichroic brownish green plates, which were washed with hexane, dried, and used for single crystal XRD analysis**.**

‡ *Crystal data for* **1**. M = 835.54, monoclinic, space group $C2/c$, a = = 33.0928(17), b = 10.5093(5) and c = 23.0334(12) Å, β = = 133.6200(10)°, V = 5799.1(5) Å^3, Z = 8, T = 120(2) K, μ(MoKα) = = 3.823 mm^{-1}, d_{calc} = 1.914 g cm^{-3}, 34860 reflections measured (4.232° ⩽ 2θ ⩽ 57.998°), 7687 unique (R_{int} = 0.0303, R_σ = 0.0234) which were used in all calculations. The final R_1 was 0.0437 ($I > 2\sigma(I)$) and wR_2 was 0.1153 (all data).

Crystal data for **2**. M = 926.99, triclinic, space group $P\bar{1}$, a = 11.0247(3), b = 11.5388(3) and c = 13.0174(3) Å, α = 86.1080(10)°, β = 80.0180(10)°, γ = 71.7630(10)°, V = 1548.82(7) Å^3, Z = 2, T = 296 K, μ(MoKα) = 4.489 mm^{-1}, d_{calc} = 1.988 g cm^{-3}, 29066 reflections measured (4.514° ⩽ 2θ ⩽ 56.998°), 7786 unique (R_{int} = 0.0441, R_σ = 0.0455), which were used in the calculations. The final R_1 was 0.0391 ($I > 2\sigma(I)$) and wR_2 was 0.0694 (all data).

Crystal data for **3**. M = 706.99, triclinic, space group $P\bar{1}$ (no. 2), a = 7.8909(2), b = 8.9494(2) and c = 9.4015(3) Å, α = 63.5740(10)°, β = 89.3160(10)°, γ = 87.6300(10)°, V = = 594.03(3) Å^3, Z = 1, T = 150.0 K, μ(MoKα) = 4.533 mm^{-1}, d_{calc} = = 1.976 g cm^{-3}, 11936 reflections measured (4.838° ⩽ 2θ ⩽ 65.234°), 3535 unique (R_{int} = 0.0308, R_σ = 0.0334) which were used in all calculations. The final R_1 was 0.0281 ($I > 2\sigma(I)$) and wR_2 was 0.0519 (all data).

A Bruker SMART CCD area detector diffractometer with a graphite-monochromated MoKα radiation (0.71070 Å) was used for the cell determination and intensity data collection for compounds **1**–**3**. The structure was solved by direct methods and refined by full-matrix least squares against F^2 using the SHELXL and Olex2 software. Nonhydrogen atoms were refined with anisotropic thermal parameters. All hydrogen atoms were geometrically fixed and refined using a riding model.

CCDC 1990935–1990937 contain the supplementary crystallographic data for this paper. These data can be obtained free of charge from The Cambridge Crystallographic Data Centre *via* http://www.ccdc.cam.ac.uk.

§ See details in Online Supplementary Materials.

¶ The intermolecular energies were calculated in CrystalExplorer 17.5 (TONTO, B3LYP-DGDZVP) for all unique molecular pairs in the first coordination sphere of a molecule using experimental crystal geometries.

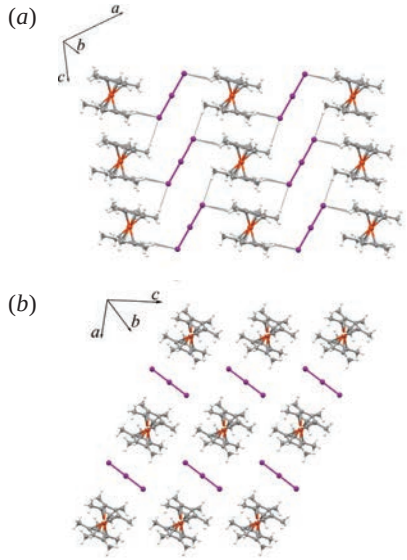

Figure 4 Fragments of the solid state structure of two polymorphic forms of [DMFc]I_3 (**3a**, **3b**). Notice a different direction of I_3 anions.

the orthogonal dimension[18] to the I···DMFc in the parent crystal of [$DMFc^+$]I_3.[11,12]

The energies of O–H···I–I_2 HBs and 4-XC_6H_4OH–DMFc stacking are comparable, while the energy of predominantly ionic interactions between $[DMFc]^+$ and $[I_3]^-$ exceeds them by a factor of 5 to 6 [–181/–238 kJ mol^{-1} (**1**), –190/–242/–260 kJ mol^{-1} (**2**)] and is very close to those in $[DMFc]^+[I_3]^-$ (–180/–238 kJ mol^{-1}). Along with this, a comparison of repulsive intermolecular interactions in starting [DMFc][I_3] and **1**, **2** indicated a decrease of the repulsion between its like charges on addition of the third neutral co-former to the ionic crystal.§ This apparently contributes to the energetic profit of the formation of $[A^-]$–B–$[C^+]$ cocrystals from $[A^-][C^+]$.

Finally, note that [DMFc][I_3] does not result in salt cocrystals with 1,4-hydroquinone, as could be expected by analogy of 1,4-hydroquinone with 4-ClC_6H_4OH and analysis of HB/XB interactions in **1**, but it afforded a new polymorphic form of [DMFc][I_3] ($P\bar{1}$, **3b**) under the same conditions. In contrast to the known $C2/m$ form of [DMFc][I_3] (**3a**),[7] the I_3 anions in **3b** are orthogonal to the Cp*–Fe–Cp* axis (Figure 4).

The existence of such polymorphic forms of [DMFc][I_3] with a notable difference in the directions of I_3 anions is another argument in favor of a low structure-forming contribution of strong ionic bonding.

The energies of hydrogen, halogen, and π-π stacking interactions (~10 kcal mol^{-1}) may seem unnoticeable in the shadow of a fivefold stronger ionic bonding (~50 kcal mol^{-1}) in **1** and **2**; nevertheless, these relatively weak directional and specific interactions are directing the supramolecular architecture of such a three-component system in a significant and somewhat predictable way. This conclusion is consistent with the results of a topological analysis of theoretical electron density distribution in the series of cocrystals of the neutral high-energetic material CL-20†† with ionic liquids,[19] and invariom *vs.* conventional charge density analysis of high-resolution XRD in the crystals of guanidinium chloride and carbonate salts,[20] indicating the significance of weak interactions in the packing of ionic crystals.

This work was supported by the Russian Science Foundation (grant no. 19-13-00338). The XRD experiments were performed using the equipment of shared experimental facilities supported by N. S. Kurnakov Institute of General and Inorganic Chemistry, Russian Academy of Sciences.

Online Supplementary Materials

Supplementary data associated with this article can be found in the online version at doi: 10.1016/j.mencom.2020.09.009.

References

1 C. B. Aakeröy, M. E. Fasulo and J. Desper, *Mol. Pharmaceutics*, 2007, **4**, 317.
2 S. L. Childs, G. P. Stahly and A. Park, *Mol. Pharmaceutics*, 2007, **4**, 323.
3 S. Aitipamula, R. Banerjee, A. K. Bansal, K. Biradha, M. L. Cheney, A. R. Choudhury, G. R. Desiraju, A. G. Dikundwar, R. Dubey, N. Duggirala, P. P. Ghogale, S. Ghosh, P. K. Goswami, N. R. Goud, R. R. K. R. Jetti, P. Karpinski, P. Kaushik, D. Kumar, V. Kumar, B. Moulton, A. Mukherjee, G. Mukherjee, A. S. Myerson, V. Puri, A. Ramanan, T. Rajamannar, C. M. Reddy, N. Rodriguez-Hornedo, R. D. Rogers, T. N. G. Row, P. Sanphui, N. Shan, G. Shete, A. Singh, C. C. Sun, J. A. Swift, R. Thaimattam, T. S. Thakur, R. Kumar Thaper, S. P. Thomas, S. Tothadi, V. R. Vangala, N. Variankaval, P. Vishweshwar, D. R. Weyna and M. J. Zaworotko, *Cryst. Growth Des*., 2012, **12**, 2147.
4 A. Mukherjee, *Cryst. Growth Des*., 2015, **15**, 3076.
5 P. Ganguly and G. R. Desiraju, *CrystEngComm*, 2010, **12**, 817.
6 G. R. Desiraju, *Angew. Chem., Int. Ed. Engl.*, 1995, **21**, 2311.
7 C. J. Horn, A. J. Blake, N. R. Champness, A. Garau, V. Lippolis, C. Wilson and M. Schröder, *Chem. Commun*., 2003, 312.
8 M. C. Aragoni, M. Arca, C. Caltagirone, C. Castellano, F. Demartin, A. Garau, F. Isaia, V. Lippolis, R. Montis and A. Pintus, *CrystEngComm*, 2012, **14**, 5809.
9 K.-F. Tebbe and R. Buchem, *Z. Anorg. Allg. Chem.*, 1998, **624**, 671.
10 P. G. Jones and C. Muller, *Z. Kristallogr.*, 1995, **210**, 895.
11 D. Sharada, V. G. Saraswatula and B. K. Saha, *Cryst. Growth Des.*, 2018, **18**, 3719.
12 S. Tothadi and G. R. Desiraju, *Chem. Commun.*, 2013, **49**, 7791.
13 C. Gamekkanda, A. S. Sinha, J. Desper, M. Đaković and C. B. Aakeröy, *New J. Chem.*, 2018, **13**, 10539.
14 G. R. Desiraju and R. Parthasarathy, *J. Am. Chem. Soc*., 1989, **111**, 8725.
15 Y. V. Torubaev, I. V. Skabitskiy, P. Rusina, A. A. Pasynskii, D. K. Rai and A. Singh, *CrystEngComm*, 2018, **20**, 2258.
16 Y. V. Torubaev and I. V. Skabitskiy, *CrystEngComm*, 2019, **46**, 7057.
17 G. Bolla and A. Nangia, *Chem. Commun*., 2015, **51**, 15578.
18 F. Topić and K. Rissanen, *J. Am. Chem. Soc*., 2016, **20**, 6610.
19 I. V. Fedyanin, K. A. Lyssenko, L. L. Fershtat, N. V. Muravyev and N. N. Makhova, *Cryst. Growth Des.*, 2019, **19**, 3660.
20 Y. V. Nelyubina and K. A. Lyssenko, *Chem. – Eur. J*., 2015, **21**, 9733.

Received: 19th June 2020; Com. 20/6241

†† CL-20 or HNIW: 2,4,6,8,10,12-hexanitro-2,4,6,8,10,12-hexaazaisowurtzitane.